HOKKAIDO UNIVERSITY

Title	Luminescence of a Cooper Pair
Author(s)	Asano, Yasuhiro; Suemune, Ikuo; Takayanagi, Hideaki; Hanamura, Eiichi
Citation	Physical Review Letters, 103(18), 187001 https://doi.org/10.1103/PhysRevLett.103.187001
Issue Date	2009-10
Doc URL	http://hdl.handle.net/2115/45362
Rights	© 2009 The American Physical Society
Type	article
File Information	289_suemune.pdf

Luminescence of a Cooper Pair

Yasuhiro Asano,[1,2] Ikuo Suemune,[3,4] Hideaki Takayanagi,[4,5,6] and Eiichi Hanamura[7]

[1]*Department of Applied Physics, Hokkaido University, Sapporo 060-8628, Japan*
[2]*Center of Education & Research for Topological Science & Technology, Hokkaido University, Sapporo 060-8628, Japan*
[3]*Research Institute for Electronic Science, Hokkaido University, Sapporo 001-0021, Japan*
[4]*CREST, Japan Science and Technology Agency, Kawaguchi 332-0012, Japan*
[5]*Department of Applied Physics, Tokyo University of Science, Tokyo 162-8601, Japan*
[6]*International Center for Nanoarichitectonics, NIMS, Tsukuba 305-0044, Japan*
[7]*Japan Science and Technology Agency, Kawaguchi 332-0012, Japan*
(Received 6 May 2009; published 30 October 2009)

This Letter theoretically discusses the photon emission spectra of a superconducting *p-n* junction. On the basis of the second order perturbation theory for electron-photon interaction, we show that the recombination of a Cooper pair with two *p*-type carriers causes enhancement of the luminescence intensity. The calculated results of photon emission spectra explain characteristic features of observed signal in an recent experiment. Our results indicate high functionalities of superconducting light-emitting devices.

Light-emitting diodes (LEDs) usually fabricated on semiconductors have been an important element of modern technologies. Recent researches seem to focus on producing a well controlled photon and an entangled photon pair [1,2] for realizing quantum information. Superconducting devices have a great advantage in producing entangled quantum states because of its coherent nature [3–5]. Superconducting LEDs [6] have been originally proposed in the context of superradiation. Today, they are a promising source of an entangled photon pair [7]. A recent theoretical study predicts the Josephson radiation in a superconducting *p-n* junction [8]. Thus hybrids of superconductor and semiconductor LED undoubtedly have a possibility to provide a key technology in the next generation.

The radiative recombination of Cooper pairs has been observed recently in a InGaAs/InP *p-n* junction attaching onto a superconductor Nb [9]. The electroluminescence becomes drastically large at low temperatures below the superconducting transition temperature T_c of Nb electrode. Surprisingly the degree of enhancement in the luminescence intensity is 1 order of magnitude. Although the experiment has shown clearly effects of superconductivity on the radiative recombination, the mechanism has been an open question. This Letter theoretically addresses this issue. We study the emission spectra of photon in a superconducting *p-n* junction by using the second order perturbation expansion for electron-photon interaction. In the second order, we find that a peculiar recombination process to superconductivity enhances the luminescence intensity. In that recombination process, two electrons recombine with two *p*-type carriers as a Cooper pair. The theoretical results explain characteristic features of the experimental findings [9]. This Letter not only figures out a mechanism of the large luminescence intensity but also gives a guide

for designing highly functional superconducting light-emitting devices.

Let us consider a *p*-type semiconductor-superconductor junction under the applied bias voltage eV_{sd} as shown in Fig. 1(a). The energy is measured from the horizontal line indicated by "0". The sign of energy in a *p*-type semiconductor is chosen to be opposite to that in a superconductor. We assume that a semiconductor and a superconductor are in their local equilibrium which are characterized by the local chemical potential μ_p and μ_n, respectively. The edges of the conduction and valence bands are E_c and E_v, respectively. In what follows, we use a unit of $\hbar = k_B = c = 1$, where k_B is the Boltzmann constant and c is
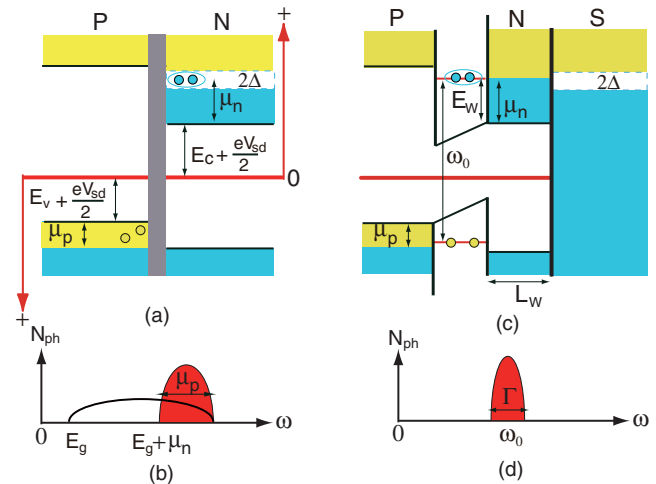

FIG. 1 (color online). Schematic energy diagram of forward biased *p-n* junctions. A theoretical model used for calculation is shown in (a). In (c), a realistic junction in experiments is illustrated. Predicted results of the photon spectra are shown in (b) and (d).

the speed of light. The p-type semiconductor is described by

$$H_p = \sum_{k,\sigma} \epsilon_p(k) b_{k,\sigma}^\dagger b_{k,\sigma}, \qquad (1)$$

where $\epsilon_p(k) = k^2/(2m_p) + E_v + eV_{sd}/2$, m_p is the effective mass, and $b_{k,\sigma}^\dagger (b_{k,\sigma})$ is the creation (annihilation) operator of a p-type carrier with a wave number k and spin $\sigma = \uparrow$ or $\downarrow$. The photon states are described by

$$H_{\mathrm{ph}} = \sum_q \omega_q \left(a_q^\dagger a_q + \frac{1}{2} \right), \qquad (2)$$

where $a_q^\dagger (a_q)$ is the creation (annihilation) operator of a photon with a wave number q and an energy ω_q. The normal state in a metal is described by

$$H_{nn} = \sum_{k,\sigma} \left(\frac{k^2}{2m_n} + E_c + \frac{eV_{sd}}{2} \right) c_{k,\sigma}^\dagger c_{k,\sigma}, \qquad (3)$$

where $c_{k,\sigma}^\dagger (c_{k,\sigma})$ is the creation (annihilation) operator of an n-type carrier and m_n is the effective mass. The electron-photon interaction Hamiltonian in the dipole approximation is given by

$$H_I = \sum_{k,q,\sigma} B_{k,q} b_{k-q,\sigma} c_{k,\sigma} a_q^\dagger + \mathrm{H.c.}, \qquad (4)$$

where $B_{k,q}$ is the coupling energy. On the basis of the second order perturbation theory, the number of emitting photon $N_{\mathrm{ph}} = \sum_q a_q^\dagger a_q$ is calculated as

$$\langle N_{\mathrm{ph}} \rangle = \langle N_{\mathrm{ph}}(1) \rangle + \langle N_{\mathrm{ph}}(2) \rangle, \qquad (5)$$

$$\langle N_{\mathrm{ph}}(1) \rangle = \int_{-\infty}^t dt_1 \int_{-\infty}^t dt_2 \langle \chi_0 | H_I(t_1) N_{\mathrm{ph}} H_I(t_2) | \chi_0 \rangle, \qquad (6)$$

$$\langle N_{\mathrm{ph}}(2) \rangle = \int_{-\infty}^{t_2} dt_1 \int_{-\infty}^t dt_2 \int_{-\infty}^t dt_3 \int_{-\infty}^{t_3} dt_4 I(2), \qquad (7)$$

$$I(2) = \langle \chi_0 | H_I(t_1) H_I(t_2) N_{\mathrm{ph}} H_I(t_3) H_I(t_4) | \chi_0 \rangle, \qquad (8)$$

$$| \chi_0 \rangle \rightarrow | 0 \rangle \otimes | N \rangle \otimes | P \rangle, \qquad (9)$$

where $| 0 \rangle$ is the zero photon state.

The BCS theory describes superconducting states,

$$H_{ns} = \sum_{k,\sigma} E_k \gamma_{k,\sigma}^\dagger \gamma_{k,\sigma}, \qquad (10)$$

where $E_k = \sqrt{\xi_n^2(k) + \Delta^2}$, $\xi_n(k) = k^2/2m_n - \mu_n$, Δ is the pair potential, and $\gamma_{k,\sigma}^\dagger (\gamma_{k,\sigma})$ is the creation (annihilation) operator of a Bogoliubov quasiparticle. We try to consider effects of superconductivity through the Bogoliubov transformation [10]. The description in Eq. (10), however, is valid within a small energy scale near the Fermi level which is at $\tilde{\mu}_n = E_c + eV_{sd}/2 + \mu_n$ measured from 0.

To apply the BCS theory to the present issue, a rule is necessary to describe the operator in the interaction picture. The transformation connects an electron operator and Bogoliubov operators by

$$c_{k,\sigma}^\dagger(t) = e^{i\tilde{\mu}_n t} (u_k e^{iE_k t} \gamma_{k,\sigma}^\dagger - s_\sigma v_k e^{-iE_k t} \gamma_{-k,\bar{\sigma}}), \qquad (11)$$

in $\langle \chi_0 | \cdots | \chi_0 \rangle$, where $u_k(v_k) = \{[1 + (-1)\xi_n(k)/E_k]/2\}^{1/2}$, $s_\sigma = 1(-1)$ for $\sigma = \uparrow (\downarrow)$, and $\bar{\sigma}$ means the opposite spin to σ. The thermal average of operators is carried out in the local equilibrium. In a p-type semiconductor, for instance, the average of operators is calculated in

$$H_p' = \sum_{k,\sigma} \xi_p(k) b_{k,\sigma}^\dagger b_{k,\sigma}, \qquad (12)$$

instead of Eq. (1) with $\xi_p(k) = k^2/2m_p - \mu_p$. In a superconductor, the average of the Bogoliubov operators is calculated in Eq. (10). In Eq. (9), $|P\rangle$ means the state vector of p-type carrier in the local equilibrium and $|N\rangle$ indicates the BCS state in the local equilibrium.

The time average of the photon number $\overline{\langle N_{\mathrm{ph}} \rangle}$ corresponds to the luminescence intensity and it in the first order perturbation expansion results in

$$\overline{\langle N_{\mathrm{ph}}(1) \rangle} = 2\pi \sum_{k,q,\sigma} |B_{k,q}|^2 f_{k-q}^p [u_k^2 f_k^n \delta(\tilde{\omega} - E_k) \\ + v_k^2 (1 - f_k^n) \delta(\tilde{\omega} + E_k)], \qquad (13)$$

where $\tilde{\omega} = \omega_q - E_g - \mu_n - \mu_p - \xi_p(k - q)$, $E_g = E_v + E_c + eV_{sd}$, $f_k^n = [1 - \tanh(E_k/2T)]/2$, and $f_k^p = \{1 - \tanh[\xi_p(k)/2T]\}/2$. This result recovers the photon spectra in a normal p-n junction by tuning $\Delta \rightarrow 0$, which means that $E_k \rightarrow -\xi_n(k)$, $u_k \rightarrow 0$, $v_k \rightarrow 1$ for $k < k_F$ and $E_k \rightarrow \xi_n(k)$, $u_k \rightarrow 1$, $v_k \rightarrow 0$ for $k > k_F$ with k_F being the Fermi wave number satisfying $k_F^2/2m_n = \mu_n$. The threshold of spectra is E_g and the width of spectra is given by $\mu_n + \mu_p$. The spectra in Eq. (13) have a broad profile reflecting the quasiparticle density of states as schematically shown in Fig. 1(b). Equation (13) depends on temperature through the Fermi distribution function and the pair potential. We have, however, numerically confirmed that the dependence is very weak and that Eq. (13) is almost constant below and near above T_c. The general features of spectra are determined by the energy scales such as E_g, μ_n, and μ_n. They are much larger than Δ.

The results of the second order perturbation are given by

$$I(2) = \sum_{k_1 \cdots k_4, q_1 \cdots q_4, \sigma_1 \cdots \sigma_4} e^{-i\Omega_1 t_1 - i\Omega_2 t_2 + i\Omega_3 t_3 + i\Omega_4 t_4} \\ \times B_{k_1,q_1}^* B_{k_2,q_2}^* B_{k_3,q_3} B_{k_4,q_4} Q_{Ph} Q_P Q_N, \qquad (14)$$

with $\Omega_j(k_j, q_j) = \omega_{q_j} - \epsilon_P(k_j - q_j) - \tilde{\mu}_n$. The average of the operators Q_{Ph}, Q_P, and Q_N are calculated as follows,

$$Q_{Ph} = \sum_{q_5} \langle 0 | a_{q_1} a_{q_2} a_{q_5}^\dagger a_{q_5} a_{q_3}^\dagger a_{q_4}^\dagger | 0 \rangle \\ = 2(\delta_{14}^q \delta_{23}^q + \delta_{13}^q \delta_{24}^q), \qquad (15)$$

$$Q_P = \langle P|b^\dagger_{p_1,\sigma_1} b^\dagger_{p_2,\sigma_2} b_{p_3,\sigma_3} b_{p_4,\sigma_4}|P\rangle,$$

$$= f^p_{p_1} f^p_{p_2}(\delta^\sigma_{14}\delta^\sigma_{23}\delta^p_{14}\delta^p_{23} - \delta^\sigma_{13}\delta^\sigma_{24}\delta^p_{13}\delta^p_{24}), \quad (16)$$

where $\delta^q_{ij} = \delta_{q_i,q_j}$, $\delta^\sigma_{ij} = \delta_{\sigma_i,\sigma_j}$, $\delta^p_{ij} = \delta_{p_i,p_j}$, and $p_j = k_j - q_j$. By applying the Bogoliubov transformation, we find,

$$Q_N = \langle N|(u_{k_1} e^{iE_{k_1} t_1} \gamma^\dagger_{k_1,\sigma_1} - \sigma_1 v_{k_1} e^{-iE_{k_1} t_1} \gamma_{-k_1,\bar\sigma_1})$$

$$\times (u_{k_2} e^{iE_{k_2} t_2} \gamma^\dagger_{k_2,\sigma_2} - \sigma_2 v_{k_2} e^{-iE_{k_2} t_2} \gamma_{-k_2,\bar\sigma_2})$$

$$\times (u_{k_3} e^{-iE_{k_3} t_3} \gamma_{k_3,\sigma_3} - \sigma_3 v_{k_3} e^{iE_{k_3} t_3} \gamma^\dagger_{-k_3,\bar\sigma_3})$$

$$\times (u_{k_4} e^{-iE_{k_4} t_4} \gamma_{k_4,\sigma_4} - \sigma_4 v_{k_4} e^{iE_{k_4} t_4} \gamma^\dagger_{-k_4,\bar\sigma_4})|N\rangle,$$

$$(17)$$

which gives 12 terms. In what follows, we extract the most dominant contribution in Eq. (17). The average of Q_N includes the following four terms

$$Q_N(S) = u_{k_1} v_{k_1} u_{k_3} v_{k_3} \delta_{\sigma_1,\bar\sigma_2} \delta_{\sigma_3,\bar\sigma_4} \delta_{k_1,-k_2}$$

$$\times \delta_{k_3,-k_4} \sigma_1 \sigma_3 [e^{iE_{k_1}(t_1-t_2)} e^{-iE_{k_3}(t_3-t_4)} f^n_{k_1}(1 - f^n_{k_3})$$

$$+ e^{-iE_{k_1}(t_1-t_2)} e^{iE_{k_3}(t_3-t_4)} f^n_{k_3}(1 - f^n_{k_1})$$

$$- e^{-iE_{k_1}(t_1-t_2)} e^{-iE_{k_3}(t_3-t_4)} (1 - f^n_{k_1})(1 - f^n_{k_3})$$

$$- e^{iE_{k_1}(t_1-t_2)} e^{iE_{k_3}(t_3-t_4)} f^n_{k_1} f^n_{k_3}]. \quad (18)$$

Equation (18) describes effects of superconductivity on the emission spectra because $\delta_{\sigma_3,\bar\sigma_4}\delta_{k_3,-k_4}$ means the destruction of two electrons as a Cooper pair. A recombination process in $Q_N(S)$ is schematically illustrated in Fig. 2(a). The remaining eight terms in Q_N describe the emitting processes shown in Fig. 2(b) and give the luminescence intensity proportional to $\overline{\langle N_{\rm ph}(1)\rangle}^2$. We will show that $Q_N(S)$ gives large contribution to the emission spectra at $\delta q = q_1 + q_2 = 0$ ($\delta q = q_3 + q_4 = 0$ in other words)
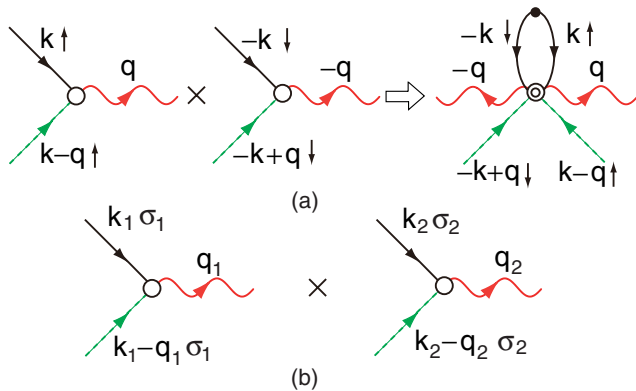

(a)

(b)

FIG. 2 (color online).   Recombination processes in the second order perturbation expansion, where solid, broken, and wavy lines represent the propagation of an electron, a p-type carrier, and a photon, respectively. In (a), a recombination of a Cooper pair in $Q_N(S)$ is shown. In (b), a recombination process other than $Q_N(S)$ is illustrated.

[11]. Substituting Eqs. (15), (16), and (18) into Eq. (14) and carrying out time integrations, we obtain

$$\overline{\langle N_{\rm ph}(2)\rangle} = 4\pi|B|^4 \sum_{q,\sigma} \delta(\Omega_{k_F,q}) I_0, \quad (19)$$

$$I_0 = \sum_k \left[\frac{f^n_k(1 - f^n_k)}{(E_k - i/\tau)^2} + \frac{f^n_k(1 - f^n_k)}{(E_k + i/\tau)^2}\right.$$

$$\left. + \frac{(f^n_k)^2 + (1 - f^n_k)^2}{E_k^2 + (1/\tau)^2}\right]\frac{\Delta^2}{E_k^2}, \quad (20)$$

where a relaxation time τ is introduced to remove effects of the perturbation at $t \to -\infty$. We neglect dependence of B on wave numbers and assume $f^p_{k_F-q} = 1$. At $1/\tau = 0$, $I_0 = \pi N_0/2\Delta$ essentially diverges for small Δ with N_0 denoting the normal density of states in a superconductor at the Fermi energy. The singular behavior at small Δ in Eq. (20) is a sign of the large luminescence intensity due to superconductivity.

We first show mathematical reasons of the singularity. Then we will discuss the physics behind the phenomenon. A two-photon emitting process in $Q_N(S)$ is illustrated in Fig. 2(a). The annihilation of a Cooper pair is described by $c_{-k,\downarrow} c_{k,\uparrow}$ which includes an operator $\gamma^\dagger_{k,\uparrow} \gamma_{k,\uparrow}$. Let us assume that the energy of the initial state is zero. In the first order expansion, the operation of $\gamma_{k,\uparrow}$ to the BCS state decreases energy by $E_k + \tilde\mu_n$. At the same time, a p-type carrier with energy $\epsilon_p(k - q)$ is destroyed and a photon with energy ω_q is created. Thus the energy of the intermediate state δE_1 results in $\delta E_1 = \omega_q - \epsilon_p(k - q) - E_k - \tilde\mu_n = \Omega_{k,q} - E_k$. In the perturbation expansion, δE_1 becomes the energy denominator. In the second order, the operation of $\gamma^\dagger_{k,\uparrow}$, the destruction of a p-type carrier, and the creation of a photon gain energy by $E_k - \tilde\mu_n$, $-\epsilon_p(-k + q)$, and ω_{-q}, respectively. Therefore the difference in energy between the intermediate state and the final one becomes $\delta E_2 = \omega_q - \epsilon_p(k - q) + E_k - \tilde\mu_n = \Omega_{k,q} + E_k$. The perturbation theory requires the energy conservation between the initial state and the final one (i.e., $\delta E_1 + \delta E_2 = 0$), which leads to $2\Omega_{k,q} = 0$. As a result, a small value of E_k remains in the denominator as shown in Eq. (20). The physics behind the phenomena is simple. The BCS state has an ability to emit a pair of photons with remaining in its state almost unchanged because the BCS state is the eigenstate of $\gamma^\dagger_{k,\uparrow} \gamma_{k,\uparrow}$. The equation $\Omega_{k_F,q} = 0$ describes the emitting condition of two photons. The threshold and width of spectra are $E_g + \mu_n$ and μ_p, respectively. In Fig. 1(b), we schematically show predicted spectra in the second order process.

The singular behavior in perturbation expansion implies an importance of higher order terms for predicting the luminescence intensity quantitatively. Here we do not discuss this issue, but choose an alternative way of regularizing the obtained results. In what follows, we introduce a finite relaxation time. First we consider a mean free time
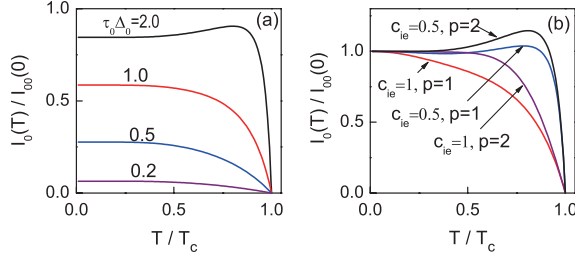
FIG. 3 (color online). Temperature dependence of lumines-
cence intensity in Eqs. (19) and (20). In (a), we consider relax-
ation time due to the elastic impurity scatterings by $\alpha = \tau_0\Delta_0$.
In (b), we consider the relaxation due to inelastic scatterings.

due to elastic impurity scatterings τ_0. At $T = 0$, we obtain
$I_0 = I_{00}(0)2\alpha^2/(\sqrt{1 + \alpha^2}(\alpha + \sqrt{1 + \alpha^2}))$, where $\alpha = \tau_0\Delta_0$, Δ_0 is the pair potential at the zero temperature and
$I_{00}(0) = \pi N_0/2\Delta_0$ is Eq. (20) at $T = 0$ and $1/\tau = 0$. At
$T \lesssim T_c$, we find

$$\frac{I_0}{I_{00}(0)} \approx \begin{cases} c_0\alpha^2(\Delta/\Delta_0)^2\Delta_0/T & \alpha \lesssim 1, \\ \alpha^3(\Delta/\Delta_0)^2 & \alpha \gg 1, \end{cases} \quad (21)$$

where c_0 is a constant of the order of unity. In Fig. 3(a), we
show I_0 as a function of temperature for several choices of
α, where we describe the dependence of Δ on temperature
by the BCS theory. The amplitude of I_0 at $T = 0$ is sup-
pressed in the dirty limit as shown in a result with $\alpha = 0.2$.
The amplitude at $T = 0$ increases with increasing α. At
$\alpha = 1$, $I_0(0)$ has almost the same amplitude as $I_{00}(0)$.
When we increase α up to 2.0, the results show a bump
just below T_c. Next we consider inelastic scatterings de-
scribed by $1/\tau_{ie} = C_{ie}(T/T_c)^p$, where C_{ie} is a coupling
constant and p depends on scattering sources such as $p =
1$ for electron-phonon scatterings and $p = 2$ for repulsive
electron-electron interaction. In Fig. 3(b), we calculate I_0
for several choices of C_{ie} and p. Since $1/\tau_{ie} \to 0$ at $T = 0$,
the amplitude is close to $I_{00}(0)$ at $T = 0$. When we de-
creases C_{ie}, the bump appears below T_c. For $1/\tau \lesssim \Delta_0$, the
luminescence intensity at $T \lesssim T_c$ is then given by

$$\overline{\langle N_{\mathrm{ph}}(2)\rangle} \approx 4\pi c_0|B|^4N_0\frac{(\tau\Delta)^2}{T}\sum_q\delta(\Omega_{k_F,q}). \quad (22)$$

Finally we modify Eq. (22) to describe the photon
spectra in realistic junctions as shown in Fig. 1(c). A
superconductor is attached to an n-type semiconductor
whose thickness L_w is about 30–50 nm [9]. The proximity
effect enables the penetration of Cooper pairs into the
n-type semiconductor. In experiments, photons are emitted
mainly from a quantum well which is sandwiched by the p-
and n-type semiconductor. The pair amplitude in the quan-
tum well can be proportional to $\Delta e^{-L_w/\xi_T}$ with $\xi_T = \sqrt{D/2\pi T}$ and D being the diffusion constant in the
n-type semiconductor. The quantum well would be re-
placed by a quantum dot near future. The level in the
quantum well (dot) E_w should coincide with the Fermi

level in the n-type semiconductor μ_n. Namely, $|E_w - \mu_n|$ must be less than both the Thouless energy $E_{\mathrm{Th}} = D/L_w^2$ and Δ. This resonant condition is particularly im-
portant for a Cooper pair to penetrate into the quantum well
(dot). The emission spectra have a peak at ω_0 and the peak
width is given by $\Gamma = t_w^2 N_0$, where t_w is the transfer
integral between the quantum well (dot) and the semicon-
ductor. The argument above is summarized by an equation
for $T \lesssim T_c$

$$\overline{\langle N_{\mathrm{ph}}(2)\rangle} \approx |B|^4N_0\Gamma\sum_{q,\sigma}\frac{\Delta^2\tau^2 e^{-2L_w/\xi_T}/T}{(\omega_q - \omega_0)^2 + (\Gamma)^2}, \quad (23)$$

where we introduce the Lorentz resonant function by hand.
In the experiment, ξ_T estimated to be 680 nm at 4 K is
much larger than L_w below T_c. Thus the theoretical results
in Fig. 3 may describe experimental results of the lumi-
nescence intensity. In fact, the experimental results of
Fig. 6(b) in Ref. [9] show a very similar line shape to
that in Fig. 3(a) with $\alpha = 1$.

In conclusion, we have studied the photon emission
spectra in a superconducting p-n junction based on the
second order perturbation theory for electron-photon inter-
action. We have found in the second order expansion that a
peculiar recombination process to superconductivity en-
hances the luminescence intensity. The theoretical results
explain temperature dependence of the luminescence in-
tensity observed in an recent experiment.

———————

[1] P. Michler, A. Kiraz, C. Becher, W. V. Schoenfeld, P. M.
    Petroff, Lidong Zhang, E. Hu, and A. Imamogulu, Science
    290, 2282 (2000).
[2] O. Benson, C. Santori, M. Pelton, and Y. Yamamoto, Phys.
    Rev. Lett. **84**, 2513 (2000).
[3] I. Chiorescu, P. Bertet, K. Semba, Y. Nakamura, C. J. P. M.
    Harmans, and J. E. Mooij, Nature (London) **431**, 159
    (2004).
[4] A. Wallraff, D. I. Schuster, A. Blais, L. Frunzio, R.-S.
    Huang, J. Majer, S. Kumar, S. M. Girvin, and R. J.
    Schoelkopf, Nature (London) **431**, 162 (2004).
[5] N. Katz, M. Ansmann, R. C. Bialczak, E. Lucero,
    R. McDermott, M. Neeley, M. Steffen, E. M. Weig,
    A. N. Cleland, J. M. Martinis, and A. N. Korotkov,
    Science **312**, 1498 (2006).
[6] E. Hanamura, Phys. Status Solidi B **234**, 166 (2002).
[7] I. Suemune, T. Akazaki, K. Tanaka, M. Jo, K. Uesugi,
    M. Endo, H. Kumano, E. Hanamura, H. Takayanagi,
    M. Yamanishi, and H. Kan, Jpn. J. Appl. Phys. **45**, 9264
    (2006).
[8] P. Recher, Y. V. Nazarov, and L. Kouwenhoven,
    arXiv:0902-4468.
[9] Y. Hayashi, K. Tanaka, T. Akazaki, M. Jo, H. Kumano,
    and I. Suemune, Appl. Phys. Express **1**, 011701 (2008).
[10] J. Unterhinninghofen, D. Manske, and A. Knorr, Phys.
    Rev. B **77**, 180509(R) (2008).
[11] The speed of light is much larger than the Fermi velocity.
    In such case, this condition becomes $|q_1| \sim |q_2|$.